Diffusion Phenomenon between Two Different Bitumens from Mechanical Analysis

Diffusion Phenomenon between Two Different Bitumens from Mechanical Analysis

Stefano Noto[1]; Salvatore Mangiafico[2]; Cédric Sauzéat[3]; Hervé Di Benedetto[4]; Elena Romeo[5]; and Gabriele Tebaldi[6]

Abstract: The use of reclaimed asphalt pavement (RAP) in hot asphalt mixtures has been investigated widely, mainly to increase the amount of RAP incorporated into new asphalt mixtures as secondary material. A key point to successfully increase the amount of RAP in mixtures is a comprehensive understanding of the blending between different bitumens, such as old and fresh bitumen. This paper introduces a mechanical model to simulate the diffusion phenomenon between two different bitumens on the basis of their rheological properties. A double-layer dynamic shear rheometer (DSR) specimen with a 25 mm diameter and 0.5 mm total thickness in plate–plate configuration was prepared by superposing two 0.25-mm-thick layers, each composed of a different bitumen. The evolution over time of the equivalent shear complex modulus of the whole double-layer specimen was investigated by performing a series of frequency sweeps at 50°C every 30 min. The time-dependent evolution of the equivalent modulus was modeled by considering an intermediate layer, composed of fully blended bitumen, at the interface between the two layers of the two base bitumens. The thickness of the intermediate layer increased as a function of time, due to diffusion. The validity of the model was confirmed by a frequency-independent thickness of the intermediate layer. Extrapolating the results, the model gives an indication of the blending of the two bitumens in the long-term, and the findings may suggest an interaction between different bitumens in asphalt mixtures containing RAP. The results are promising for the development of a more-refined mechanical model. **DOI: 10.1061/(ASCE)MT.1943-5533.0004116.**

Author keywords: Diffusion; Viscoelastic behavior; Binder blends; Dynamic shear rheometer (DSR) tests; Rheological measurements; Double-layer specimen.

Introduction

Reclaimed asphalt pavement (RAP) has been considered as a secondary raw material since the 1980s. Agencies and contractors have increased the amount of RAP in new asphalt mixtures (Bonaquist 2007), mainly using hot recycling and rejuvenators (Kandhal 1997). The use of RAP must be evaluated carefully in the mix design for asphalt mixtures. Researchers (Baaj et al. 2013; Jiménez del Barco Carrión et al. 2015; Bressi et al. 2015, 2016; Lo Presti et al. 2016; Mangiafico et al. 2013, 2019; Shirodkar et al. 2011) focused on the interaction between the fresh bitumen and the aged RAP bitumen to produce new mixtures. They defined the degree of blending, considered as homogeneous full-blend bitumen and the degree of partial blending, in which the degree of blending can vary between no interaction (black rock) and homogeneous full blend. These approaches require accurate knowledge of the mechanical properties of fresh and RAP bitumens, as well as their proportions within the final mixture and the effects of their interactions on the mechanical behavior of the mixture. Kaseer et al. (2020) performed laboratory tests on a high RAP–content asphalt mixture, adding recycling agents. They found a reduction in stiffness of the material and a higher cracking resistance. Navaro et al. (2012) assessed the degree of blending in asphalt mixtures using microscopic observations, and found that RAP clusters gradually were homogenized in the mixture with increasing the mixing time. Nahar et al. (2013) investigated the interfacing between two bitumens in contact, using atomic force microscopy. They found that the microstructure demonstrated the existence of an interface layer where the two materials interacted through diffusion.

Diffusion occurs due to a concentration gradient of different chemical species (Bokstein et al. 2005). The diffusion phenomenon in bitumens was investigated through numerical simulations (Ding et al. 2016; Cong et al. 2016; Guo et al. 2017) in which the diffusion rate was modeled as a function of the molecular weight of saturates, aromatics, resins, and asphaltenes. Karlsson et al. (2007) investigated the diffusion process, and developed a dynamic shear rheometer test. Using this test, Karlsson investigated the diffusion between RAP bitumen and fresh bitumen, and estimated the diffusion coefficient. Rad et al. (2014) implemented the test by recommending the preparation of a double-layer specimen before dynamic shear rheometer DSR testing. Due to a lack of thermal equilibrium, the procedure was shown to be not suitable for

[1]Ph.D. Student, Dept. of Engineering and Architecture Parco Area delle Scienze, Univ. of Parma, 181/A 43124, Parma, Italy; Univ. of Lyon/ENTPE, LTDS, CNRS (UMR5513) 3, Rue Maurice Audin, Vaulx-en-Velin 69120, France (corresponding author). ORCID: https://orcid.org/0000-0002-0816-4996. Email: stefano.noto@entpe.fr; stefano.noto@unipr.it

[2]Assistant Professor, Univ. of Lyon/ENTPE, LTDS, CNRS (UMR5513) 3, Rue Maurice Audin, Vaulx-en-Velin 69120, France. ORCID: https://orcid.org/0000-0003-0548-6989

[3]Professor, Univ. of Lyon/ENTPE, LTDS, CNRS (UMR5513) 3, Rue Maurice Audin, Vaulx-en-Velin 69120, France.

[4]Full Professor, Univ. of Lyon/ENTPE, LTDS, CNRS (UMR5513) 3, Rue Maurice Audin, Vaulx-en-Velin 69120, France. ORCID: https://orcid.org/0000-0001-5025-5173

[5]Assistant Professor, Dept. of Engineering and Architecture Parco Area delle Scienze, Univ. of Parma, 181/A 43124, Parma, Italy.

[6]Associate Professor, Dept. of Engineering and Architecture Parco Area delle Scienze, Univ. of Parma, 181/A 43124, Parma, Italy; Adjunct Professor, ESSIE Univ. of Florida, 365, Weil Hall, Gainesville, FL 32611.

Note. This manuscript was submitted on March 1, 2021; approved on July 19, 2021No Epub Date. Discussion period open until 0, 0; separate discussions must be submitted for individual papers. This paper is part of the ***Journal of Materials in Civil Engineering***, © ASCE, ISSN 0899-1561.

measurement at the beginning of the test. They also investigated the possibility of studying diffusion in mastics. Kriz et al. (2014) extended the experimental work developed by Karlsson et al. (2007), improving the sample preparation protocol. They also adopted an extended analytical simulation of diffusion, taking into account the main factors affecting the results, and confirmed the possibility of assessing the diffusion by rheological testing. Wu et al. (2021) proposed an experimental methodology to investigate how the diffusion process is affected by the mixing temperature during production of asphalt mixtures containing RAP. They produced an asphalt mixture in the laboratory using cubic RAP clusters from which they obtained layered bitumens by scraping the aggregate surfaces after the mixing process. The obtained wafers were tested using the DSR. Wu et al. highlighted the importance of the diffusion phenomenon for a successful recycled hot-mix asphalt production. Better knowledge of the diffusion phenomena should also allow to define the evolution of the mixtures properties during service life, in case of not perfect blending between RAP and fresh bitumens.

This paper experimentally investigated the diffusion phenomenon at 50°C between two different asphalt bitumens characterized by different viscosities. Diffusion is a temperature-dependent phenomenon, and its effect is amplified with increasing temperature. A test temperature of 50°C was chosen as a compromise between a very high temperature (able to simulate plant conditions, but not suitable for laboratory applications) and a lower temperature, at which the diffusion time could be extremely long. Based on previous studies (Karlsson et al. 2007; Rad et al. 2014; Kriz et al. 2014), a DSR test was developed, involving a series of frequency sweeps at 50°C of a sample consisting of two overlapping layers, each composed of a different bitumen. The hypothesis behind this approach is that the evolution over time of the rheological properties of the whole sample is related to the change of its structure due to the progressive blending of the two bitumens driven by diffusion.

Materials and Methods

Materials

Three different bitumens were used in this study. Bitumen B1 was a 170/220 bitumen, whereas Bitumen B2 was a 50/70. Bitumen B3 was a perfect blend of Bitumens B1 and B2 in equal proportions (50% B1 and 50% B2 by weight), obtained by mixing them for 5 min at 150°C in the laboratory. Table 1 presents the results of the standard tests conducted on the different bitumens: penetration at 25°C (CEN 2015a), softening point (CEN 2015b), viscosity at 160°C (CEN 2018), and residual penetration and softening point increment after rolling thin-film oven (RTFO) aging (CEN 2015c).

Rheometer Setup

The rheological properties of the bitumens were investigated by performing a series of frequency sweeps in an oscillatory testing mode, within the linear viscoelastic (LVE) domain, using an Anton-Paar MCR 101dynamic shear rheometer. The geometry selected for the experimental campaign was a parallel plate of 25 mm diameter (PP25) and a testing gap of 0.5 mm, using two different configurations. The first was a 0.5-mm-thick single-layer (SL) sample, whereas the second was a double-layer (DL) sample composed of two overlapping layers, each 0.25 mm thick, for a total thickness of 0.5 mm. The DSR was equipped with a Peltier plate and a Peltier hood for temperature control.

Methods

DSR tests were performed to investigate the time-dependent variations of the complex shear modulus of both single-layer and double-layer samples [Eq. (1)]. An equivalent time-dependent complex shear modulus $G^*(t)$ was defined. Its norm $|G^*(t)|$ and phase angle $\varphi(t)$ both are time dependent

$$G^*(t) = |G^*(t)|e^{i\varphi(t)} \tag{1}$$

The double-layer sample was prepared by overlapping two different bitumen layers, each adhering to either one of the two DSR plates. The structure of the double-layer sample at time $t = 0$ can be identified in Fig. 1(a), with the two layers simply contacting each other. This overlap created a structure that changed over time, considering the diffusion hypothesis. Diffusion can be defined as the transfer of the material, in the presence of a concentration gradient.

According to the diffusion hypothesis [Fig. 1(b)], the rheological behavior of the whole sample determined from the DSR test is time-dependent. This can be interpreted as the effect due to gradual growth of an intermediate layer, starting at the interface between the Layer 1 and Layer 2.

DSR tests were performed at a fixed temperature of 50°C for a testing time of 22 h for each bitumen and for each configuration, for a total of 24 experiments (Table 2).

Combinations B1, B2, and B3 for single-layer testing and B1 + B1, B2 + B2, and B3 + B3 for double-layer testing were selected to evaluate the effect of the preparation of the double-layer specimen. If the results had no difference in terms of statistical significance, the sample structure would be validated.

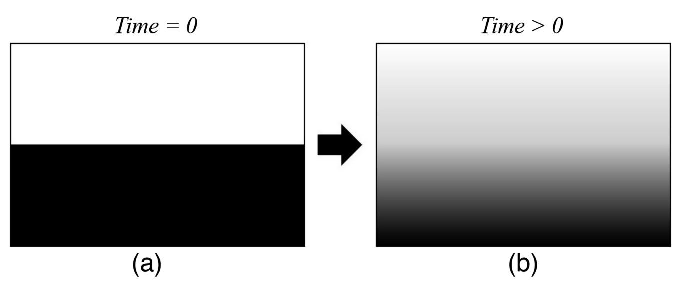

Fig. 1. Evolution over time of the sample structure: (a) time = 0, with two distinct layers put in contact; and (b) gradual blending of the two materials due to the diffusion process with time.

Table 1. Conventional tests of selected bitumens

Bitumen	Name	Penetration at 25°C (dmm)	$T_{R\&B}$ (°C)	Viscosity at 160°C (Pa · s)	Residual penetration after RTOFT (%)	$\bar{T}_{R\&B}$ After RTFOT (°C)
170/210	B1	171	49.6	0.1	65	4
50/70	B2	51	37.2	0.16	58	6
Full blend (50% B1 + 50% B2)	B3	99	45	—	—	—

Table 2. Tested specimens and number of test repetitions

Test setup	Single-layer			Double-layer			
Material	B1	B2	B3	B1 + B1	B2 + B2	B3 + B3	B1 + B2
Number of test repetitions	3	3	3	3	3	3	6

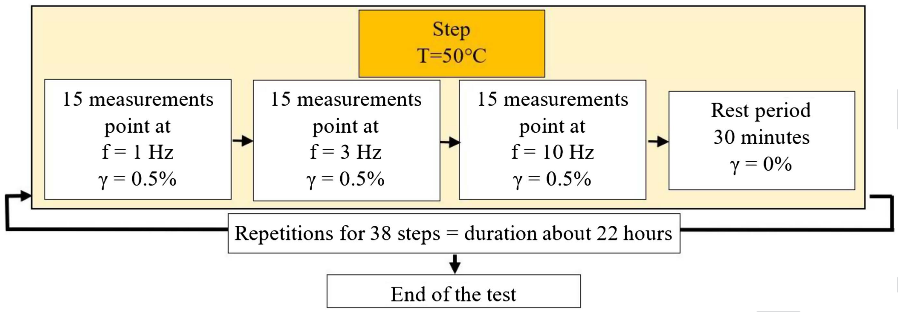

Fig. 2. Applied loading path. The test was composed of 38 repetitions at a testing temperature of 50°C. The total duration was about 22 h.

The test results obtained from the full-blend Sample B3 were compared with those obtained from the B1+B2 double layer to evaluate how far the rheological results of double-layer B1+B2 sample were from the ideal composition of the full-blend sample. This was based on the initial assumption that the two bitumens would blend, tending to a fully blended composition of the layer.

The test protocol in Fig. 2 was carried out to study the diffusion phenomenon between two different bitumens, and the rheological behavior of the double-layer samples were tested at three different frequencies (1, 3, and 10 Hz) in the linear viscoelastic domain, imposing a shear strain of 0.5%. This strain amplitude value was selected after performing two strain amplitude sweep tests on Bitumens B1 and B2. The double-layer test was composed of 38 repetitions of a load-and-rest step. Each step was composed of three measuring intervals and one resting period. During the measuring intervals, the DSR collected 15 measuring points at each tested frequency to assure reliable repetition of the same measurement. The test was performed in the Anton-Paar default mode, in which the DSR did not record raw data for each measurement point, but rather the norm of complex shear modulus and the phase angle, calculated as the average of at least three loading cycles. Moreover, the software did not specify the number of loading cycles for each measuring point.

The resting period lasted 30 min, imposing a shear strain equal to zero. The testing temperature of 50°C was chosen to observe the phenomenon at a medium-high temperature. The testing gap was fixed at 0.5 mm to avoid any leakage of bitumen and to have a shorter duration of the diffusion phenomenon, as suggested by Kriz et al. (2014). The total duration of the test procedure, 22 h, was selected to assure that the whole test procedure was completed within 24 h, including the sample preparation and the test execution. This corresponded to 38 repetitions of the steps (Fig. 2).

Sample Preparation

The sample preparation procedure was defined, starting from the procedure previously proposed by Kriz et al. (2014). This was adapted to create both double-layer samples and single-layer samples, assuring homogenous characteristics in terms of thermal history.

The double-layer sample was prepared according to the following steps. The two bitumens were heated at 150°C for 40 min, and

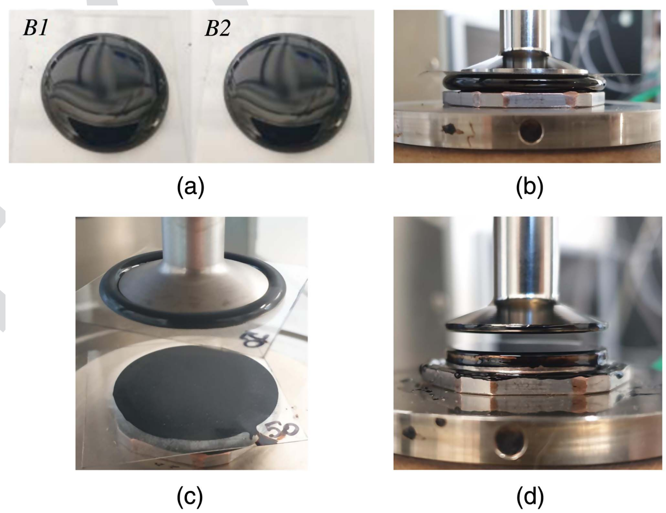

Fig. 3. DSR test setup during the preparation of the two-layer sample: (a) B1 and B2 bitumen discs on transparent films ready to be placed in the DSR; (b) B2 bitumen disc positioned on the bottom plate, with a gap of 0.362 mm (0.250 mm for bitumen + 0.100 mm for the transparent film + 0.012 mm to allow for bulge) imposed; (c) B1 bitumen disc placed onto the upper plate, with gap appropriately set to reach a total thickness of 0.725 mm (0.500 mm + 0.200 mm for the two transparent films + 0.024 mm for the bulge); and (d) after opening the hood and peeling off the two transparent films, each disc was trimmed separately, before closing the hood, conditioning at the testing temperature 50°C for 10 min, and putting samples in contact.

0.5 g Bitumen B1 was poured onto a 0.1-mm-thick transparent film square (side length = 3 cm). The same amount of Bitumen B2 then was poured onto another transparent film [Fig. 3(a)]. The two bitumen specimens were cooled and maintained at room temperature for at least 1 h. From this moment, for the rest of the test procedure, all temperature variations and conditioning were imposed using the Peltier plates and hood of the DSR. The two DSR plates were heated at 50°C for 5 min, then the zero-gap was imposed. Bitumen B2 was placed on the bottom plate with the transparent film on the top side. The material was conditioned at 50°C for 10 min.

The spindle (the upper part of the DSR measuring system) was not in contact with the transparent film during this step. The proper gap of 0.362 mm then was imposed: this gap was selected considering the target thickness of the first layer (0.250 mm), the thickness of the transparent film (0.100 mm) and the additional thickness reduction (0.012 mm) to be imposed after trimming to produce the lateral bulge of the half-sample. A normal force limit was set, with a maximum axial load allowed of 10 N [Fig. 3(b)]. The temperature then was decreased to 40°C and maintained for 10 min. This temperature was chosen because it was above the softening point of the softer bitumen, but below the softening point of the hard bitumen. The spindle was lifted, and Bitumen B1 was attached to the top plate, with the transparent film on the bottom [Fig. 3(c)]. The system then was conditioned at 40°C for 10 min. The gap of 0.724 mm was imposed, resulting from the target thickness of the first layer of Bitumen B2 (0.250 mm), the target thickness of the second layer of Bitumen B1 (0.250 mm), the total additional thickness reduction (0.025 mm) to impose after trimming both half-samples to produce the lateral bulge, and the total thickness of the two transparent films (0.200 mm). The same maximum force control limit was imposed during this phase. The temperature was decreased to −10°C and the sample was thermally conditioned for 10 min. The two transparent films were removed gently, avoiding any damage to the surfaces of the two layers of the bitumen. In the case of any damage to any of the layers, both were discarded. The temperature was increased to 20°C and maintained for 10 min. The correct thicknesses of the two layers were imposed using the process described previously. The lateral surface of the B1 layer on the top plate was trimmed carefully with a hot spatula, removing the excess bitumen. This process was performed carefully, ensuring that the hot spatula was perpendicular to the vertical axis and tangent to the lateral surface of the half sample. The trimming process was performed following the lateral shape of the spindle. The same procedure was applied to trim the B2 layer on the bottom plate. The trimming was carried out with the two layers not in contact, to avoid any undesired mixing effect caused by the trimming process. Because the two layers were not in contact during the preparation of the sample, the diffusion process did not occur before the beginning of the test.

The spindle was moved to a waiting position of 5 mm [Fig. 3(d)], and the two discs were conditioned at 50°C for 10 min using the Peltier equipment. At the end of the conditioning period, the software automatically moved the spindle to reach the final test gap of 0.500 mm. After the position was reached, the two half-samples were in contact.

The single-layer sample preparation was similar to that of the double-layer samples. The bitumen was heated at 150°C for 40 min, 0.5 g bitumen was poured onto 0.1-mm-thick transparent film square, and the disc was cooled at room temperature for at least 1 h. The two plates were heated at 50°C for 5 min, and then the zero-gap was imposed. The disc of Bitumen B2 was placed on the bottom plate with the transparent film on top. After temperature conditioning, the proper gap of 0.624 mm was imposed, including the target thickness of the disc (0.500 mm), its bulge (0.024 mm), and the thickness of the transparent film (0.100 mm). A maximum force control limit was set, with a maximum axial load of 10 N. The temperature was decreased to −10°C and the sample was conditioned for 10 min. The transparent film was removed, avoiding any damage to the disc. The temperature was increased to 20°C. After a conditioning time of 10 min, the sample was trimmed on the bottom plate with a hot spatula, ensuring that the spindle did not contact the sample, to ensure a similar procedure as for the double-layer sample preparation. The spindle was moved, imposing a waiting gap of 5 mm. The system was conditioned at 50°C for 10 min. After the temperature conditioning, the testing gap of 0.500 mm was imposed, and the sample was ready to be tested.

Experimental Results

Experimental results are presented in this section. Complex shear modulus $G^*(t)$ (norm $|G^*(t)|$ and phase angle $\varphi(t)$) are plotted as a function of time. The plotted time was zeroed at the beginning of the tests to assure a direct comparison between the tests. 12

To summarise the results, only the results obtained for Bitumen B2 are discussed, which were representative of the general trend for all three bitumens. Figs. 4–6 compare the results (average and 95% confidence intervals) obtained from three repetitions of

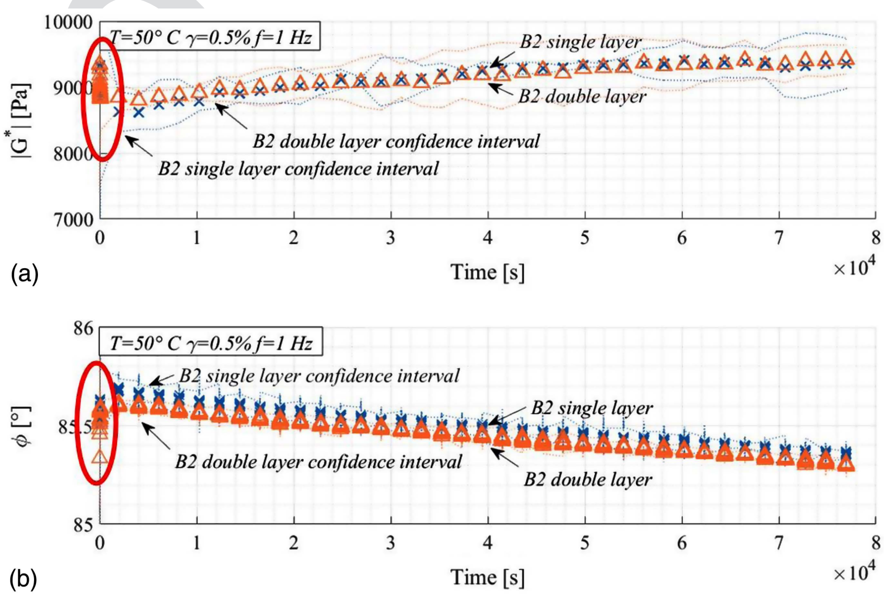

Fig. 4. Averages and confidence intervals of test results obtained for three single-layer tests of Bitumen B2 and three double-layer tests of the combination B2 + B2 at 50°C and 1 Hz: (a) norm of the complex shear modulus; and (b) phase angle.

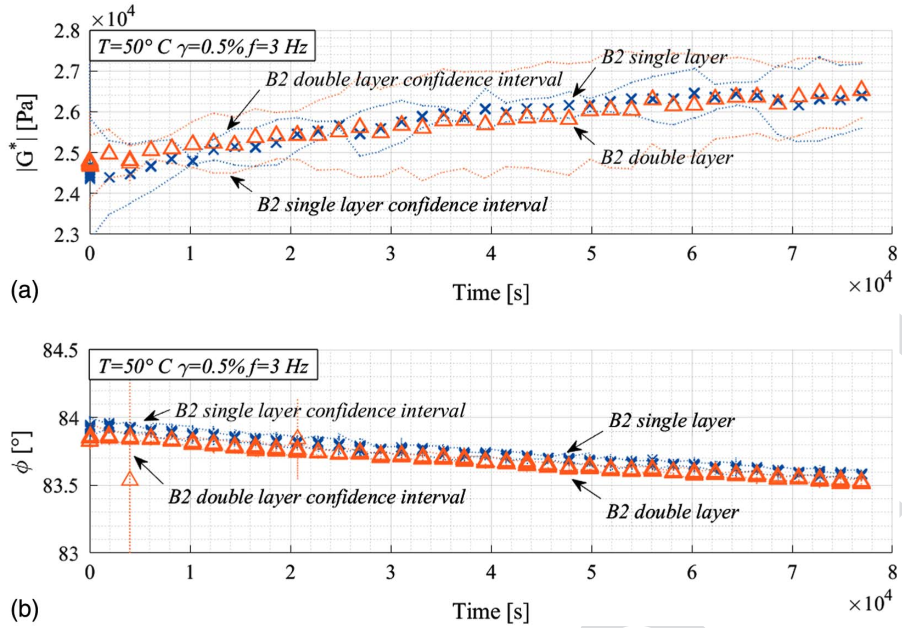

Fig. 5. Averages and confidence intervals of test results obtained for three single-layer tests of Bitumen B2 and three double-layer tests of the combination B2 + B2 at 50°C and 3 Hz: (a) norm of the complex shear modulus; and (b) phase angle.

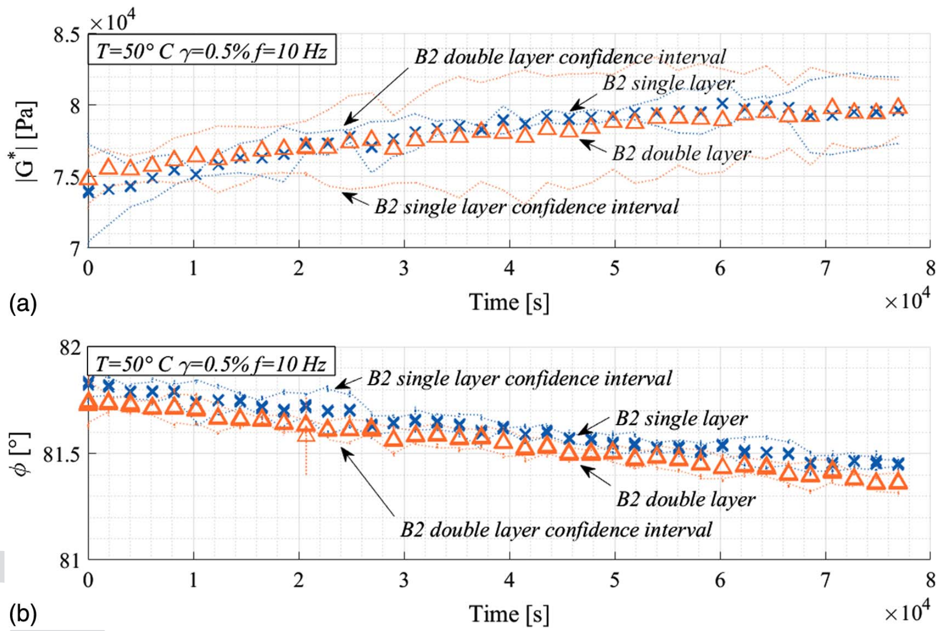

Fig. 6. Averages and confidence intervals of test results obtained for three single-layer tests of Bitumen B2 and three double-layer tests of the combination B2 + B2 at 50°C and 10 Hz: (a) norm of the complex shear modulus; and (b) phase angle.

B2 single-layer tests and three repetitions of B2 + B2 double-layer tests at 1, 3, and 10 Hz, respectively. The ovals in Fig. 4 highlight the presence of temperature regulation problems at the beginning of the tests.

The same trend occurred at the three frequencies for both types of tests. Average values of the three replicates of each test were very close, and 95% confidence intervals overlapped, showing that no relevant differences were detected. This shows that the sample typology (single- or double-layer samples of the same bitumen) did not affect the results.

The experimental results are summarized in Figs. 7–9, which show the averages and their confidence intervals for each data series of complex shear modulus (pascals) and phase angle (degrees) as a function of time (seconds). The norm of complex shear modulus [Figs. 7(a), 8(a), and 9(a)] and phase angle [Figs. 7(b), 8(b), and 9(b)] shows the experimental results at the three tested frequencies: 1, 3, and 10 Hz.

The B1, B2, and B3 data series were the results of three repetitions, each from single-layer tests. The B1 + B2 double-layer tests used a double-layer specimen, composed of Bitumen B1 on

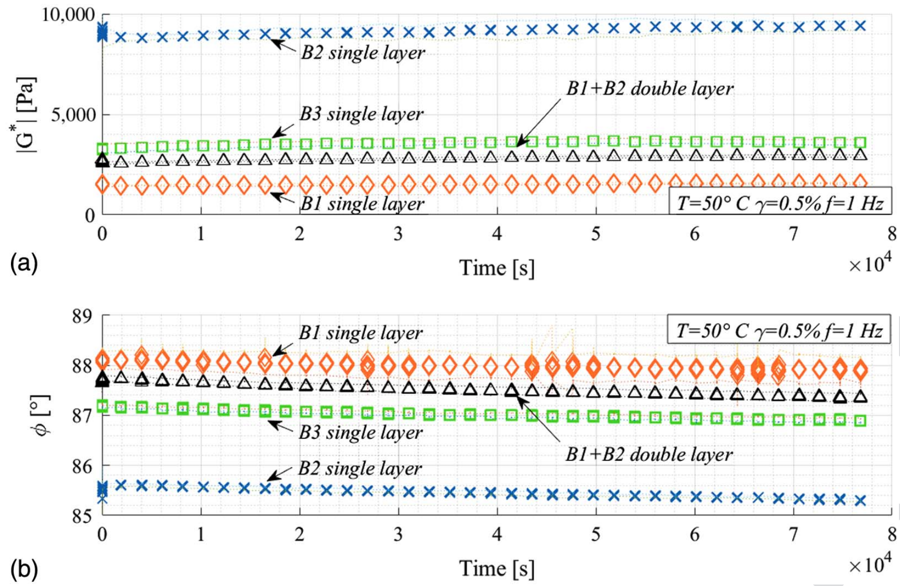

Fig. 7. Averages and confidence intervals of test results obtained for three single-layer tests of each bitumen B1, B2, and B3 and for six double-layer tests of the combination B1 + B2 at 50°C and 1 Hz: (a) norm of the complex shear modulus; and (b) phase angle.

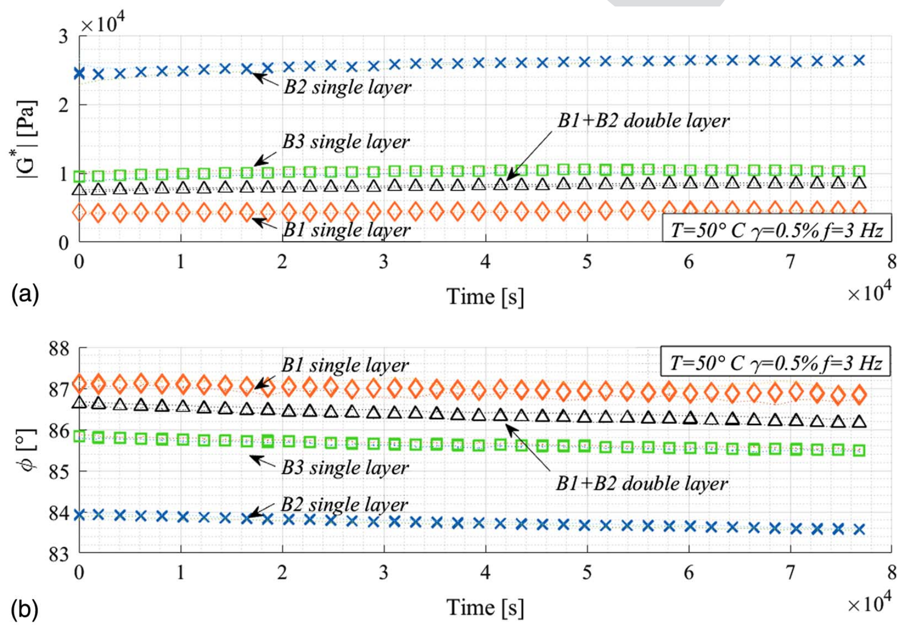

Fig. 8. Averages and confidence intervals of test results obtained for three single-layer tests of each bitumen B1, B2, and B3, and for six double-layer tests of the combination B1 + B2 at 50°C and 3 Hz: (a) norm of the complex shear modulus; and (b) phase angle.

the top layer and Bitumen B2 on the bottom layer, and considered six repetitions of the test.

The decrease of the phase angle and the increase of the norm of the shear complex modulus for the B1, B2, and B3 single-layer tests probably were due to a steric hardening phenomenon (Fig. 7).

Modeling of Results

Three-Layer Diffusion Model

A three-layer model is presented in this section, which describes the blending process driven by diffusion in a material structure composed of two different bitumen layers. The model consists in the introduction of an intermediate layer at the interface between the two B1 and B2 layers, which increases its thickness with time. This can be interpreted as the diffusion thickness, defining the region in which the diffusion is significant. The intermediate layer is considered to be composed of a homogeneous layer of Bitumen B3, which is considered to be a full blend between B1 and B2. The thickness of the intermediate layer was identified as a reliable parameter to trace the evolution of the diffusion phenomenon.

This model is based on the equivalence between the mechanical response of a homogeneous single-layer structure and a layered structure in which each layer is characterized by a thickness and a characteristic value of the norm of complex shear modulus and a phase angle.

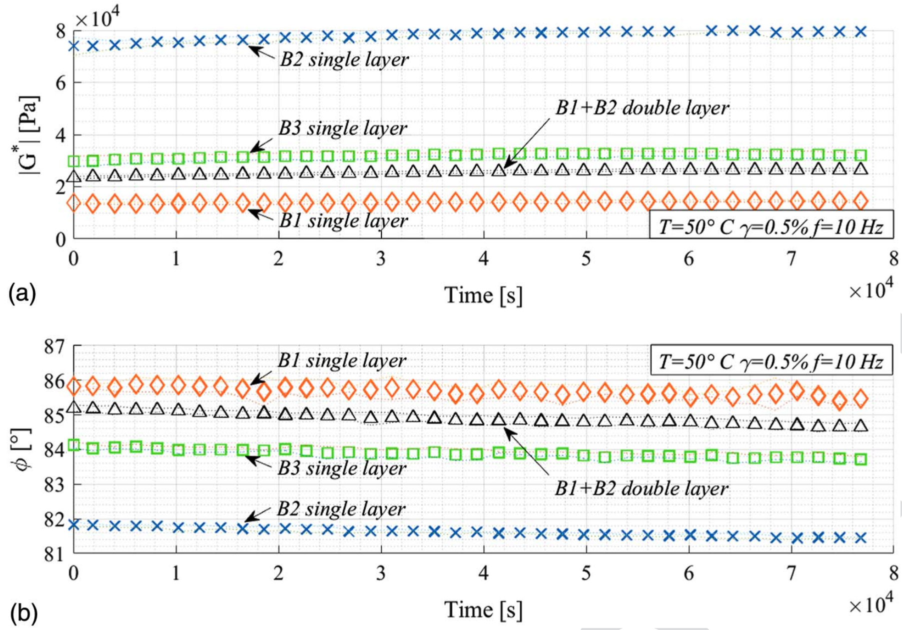

Fig. 9. Averages and confidence intervals of test results obtained for three single-layer tests of each bitumen B1, B2 and B3 and for six double-layer tests of the combination B1+B2 at 50°C and 10 Hz: (a) norm of the complex shear modulus; and (b) phase angle.

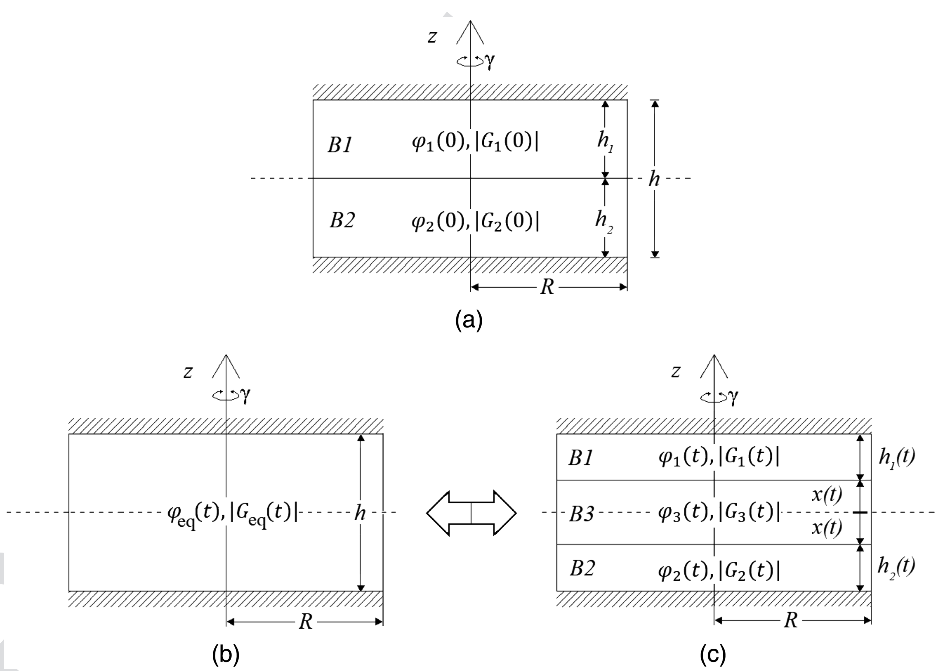

Fig. 10. Representation of the considered layers of the sample: (a) at time $t = 0$ for two layers of Bitumens B1 and B2; (b) equivalent sample structure for every time t; and (c) at time $t > 0$ for three-layer model composed of Bitumens B1 and B2 and full-blend Bitumen B3.

Fig. 10(a) shows the layered structure of the sample at time $t = 0$. Layer B1 is characterised by complex shear modulus $G_1^*(0)$ and thickness of the layer h_1. Layer B2 is characterized by $G_2^*(0)$ and h_2. The total thickness of this structure is h, defined as the sum of h_1 and h_2, and it was equal to 0.5 mm, corresponding to the total thickness of the tested samples. Fig. 10(b) represents the equivalent sample structure at any time t, in which the sample is composed of a homogeneous layer of thickness h and characterized by $G_{eq}^*(t)$ and $\varphi_{eq}(t)$. Fig. 10(c) represents the structure of the sample at a time t greater than zero. It is assumed that the structure is composed of three layers, characterized by the norms as a function of time t of the complex shear moduli $|G_1^*(t)|$, $|G_2^*(t)|$, and $|G_3^*(t)|$; phase angles $\varphi_1(t)$, $\varphi_2(t)$, and $\varphi_3(t)$; and layer thicknesses $h_1(t)$, $h_2(t)$, and $x(t)$, defined as half of the thickness of the third layer. The intermediate layer is composed of fully blended Bitumen B3, which is assumed to be generated by the diffusion phenomenon, starting from the interface between the two layers B1 and B2.

The thicknesses $h_1(t)$ and $h_2(t)$ can be defined, starting from the thicknesses of the two layers at time $t = 0$, as

$$h_1(t) = h_1 - x(t) \tag{2}$$

$$h_2(t) = h_2 - x(t) \tag{3}$$

where $x(t)$ = one-half the thickness of the intermediate layer of the third layer, composed of a full-blend Bitumen B3 [Fig. 10(c)]. The central equation of the mechanical characterization can be defined imposing the equivalence between the structure of the sample, which is considered to be composed of a homogeneous material and the layered structure [Fig. 10(b)]; the theoretical relation between the parameters is

$$\frac{h}{G^*_{eq}(t)} = \frac{h_1(t)}{G^*_1(t)} + 2\frac{x(t)}{G^*_3(t)} + \frac{h_2(t)}{G^*_2(t)} \tag{4}$$

Finally, the thickness $x(t)$ can be calculated using

$$x(t) = \frac{\frac{h}{G^*_{eq}(t)} - \frac{h_1}{G^*_1(t)} - \frac{h_2}{G^*_2(t)}}{\frac{2}{G^*_3(t)} - \frac{1}{G^*_1(t)} - \frac{1}{G^*_2(t)}} \tag{5}$$

Several terms on the right-hand side of Eq. (5) are complex numbers; therefore, real and imaginary parts have to be considered. Thickness x should be a real number, which means that the imaginary part should be null. This was checked experimentally to confirm the validity of the postulated hypotheses.

Taking into account Eq. (5), and considering the Euler identity, the real part and the imaginary part of the complex number can be defined as follows:

$$x(t) = \frac{a + ib}{c + id} \tag{6}$$

$$a = \{h_1|G^*_1|^{-1}\cos(\varphi_1) + (h - h_1)|G^*_2|^{-1}\cos(\varphi_2) - h|G^*_{eq}|^{-1}\cos(\varphi_{eq})\} \tag{7}$$

$$b = \{-h_1|G^*_1|^{-1}\sin(\varphi_1) - (h - h_1)|G^*_2|^{-1}\sin(\varphi_2) + h|G^*_{eq}|^{-1}\sin(\varphi_{eq})\} \tag{8}$$

$$c = \{|G^*_1|^{-1}\cos(\varphi_1) + |G^*_2|^{-1}\cos(\varphi_2) - 2|G^*_3|^{-1}\cos(\varphi_3)\} \tag{9}$$

$$d = \{-|G^*_1|^{-1}\sin(\varphi_1) - |G^*_2|^{-1}\sin(\varphi_2) + 2|G^*_3|^{-1}\sin(\varphi_3)\} \tag{10}$$

At time $t = 0$, Eq. (4) can be written [Fig. 10(a)]

$$\frac{h}{G^*_{eq}(0)} = \frac{h_1}{G^*_1(0)} + \frac{h_2}{G^*_2(0)} \tag{11}$$

where $h = h_1 + h_2$ = fixed gap of DSR

$$h_2 = h - h_1 \tag{12}$$

The thickness h_1 at time $t = 0$ can be evaluated according to Eq. (11), which can be found starting from Eqs. (9) and (10)

$$h_1 = h\frac{G^*_1(0)(G^*_2(0) - G^*_{eq}(0))}{G^*_{eq}(0)(G^*_2(0) - G^*_1(0))} \tag{13}$$

After the thickness h_1 is calculated using Eq. (13), the thickness h_2 can be determined, according to Eq. (12).

Analysis of Results

The experimental results were analyzed statistically. Significance levels were set at 5% using Student's t-test according to Eq. (2). Averages and confidence intervals were calculated for each data series, in which n represented the number of tests repetitions (Table 2)

$$P\left\{\bar{x} - t_{(\frac{\alpha}{2},g)}\frac{s_{\text{corr}}}{\sqrt{n}} \le \mu \le \bar{x} + t_{(\frac{\alpha}{2},g)}\frac{s_{\text{corr}}}{\sqrt{n}}\right\} = 0.95 \tag{14}$$

$$s_{\text{corr}} = \sqrt{\frac{n-1}{n}} \tag{15}$$

Experimental results were analyzed using the model described in the previous section. The thickness of the two layers at time $t = 0$ was estimated using Eq. (15).

Shear complex moduli at time $t = 0$, $G^*_1(0)$, $G^*_2(0)$, and $G^*_{eq}(0)$, were obtained by projecting the parabolic regression of the experimental data and finding the intercept of the G^* axis for time $t = 0$. Table 3 lists the results of the calculated thicknesses of the layers. The difference between the two thicknesses at time $t = 0 h_1$ and h_2 was approximately 3%.

After the two thicknesses h_1 and h_2 were evaluated, the thickness of the intermediate layer $x(t)$ was calculated using Eqs. (7) and (8). Fig. 11 shows the evolution of the thickness of $x(t)$ as a function of time for the three tested frequencies, 1 [Fig. 11(a)], 3 [Fig. 11(b)] and 10 Hz [Fig. 11(c)], displaying both the real and the imaginary parts of the model at every time t. [Fig. 11(d)] presents the result of the power-law fitting using the data obtained from all tested frequencies (1, 3, and 10 Hz).

According to the experimental results, the following observations can be drawn:

- From Fig. 11(a), $x(t = 0^+)$ was not equal to zero. This was due to a thermal regulation problem at the beginning of the tests, as can be deducted from the experimental results (Fig. 7).
- The same diffusion thickness of the intermediate layer was found for all loading frequencies [Figs. 11(a–c)]. This can be interpreted as an indication of correctness of the analysis.
- The evolution of the real part of the thickness $x(t)$ gradually increased.
- Focusing on the imaginary part of $x(t)$, the experimental results by calculations were zero for all the tested frequencies, considering experimental scattering. This is in line with the fact that $x(t)$ is defined as a physical quantity representing a thickness, which must be a real number.
- The data of the real part of $x(t)$ calculated at 1, 3, and 10 Hz were fitted with a power law regression with $R^2 = 0.957$.
- According to the findings at 50°C, the regression equation can be used to assess the duration of the diffusion process. However, this approach potentially could lead to error, due to the extrapolation process of the interval of experimental data. Diffusion could lead the double-layer structure, composed of different bitumens, to behave similarly to a perfect fully blended bitumen in the long term, because the end of the diffusion process, considered to be 95% of the half-thickness of the sample (0.25 mm), was estimated to occur at 46.6 days.

Table 3. Calculated thickness of two layers of B1 and B2 at time $t = 0$ (mm)

h_1	h_2
0.247	0.253

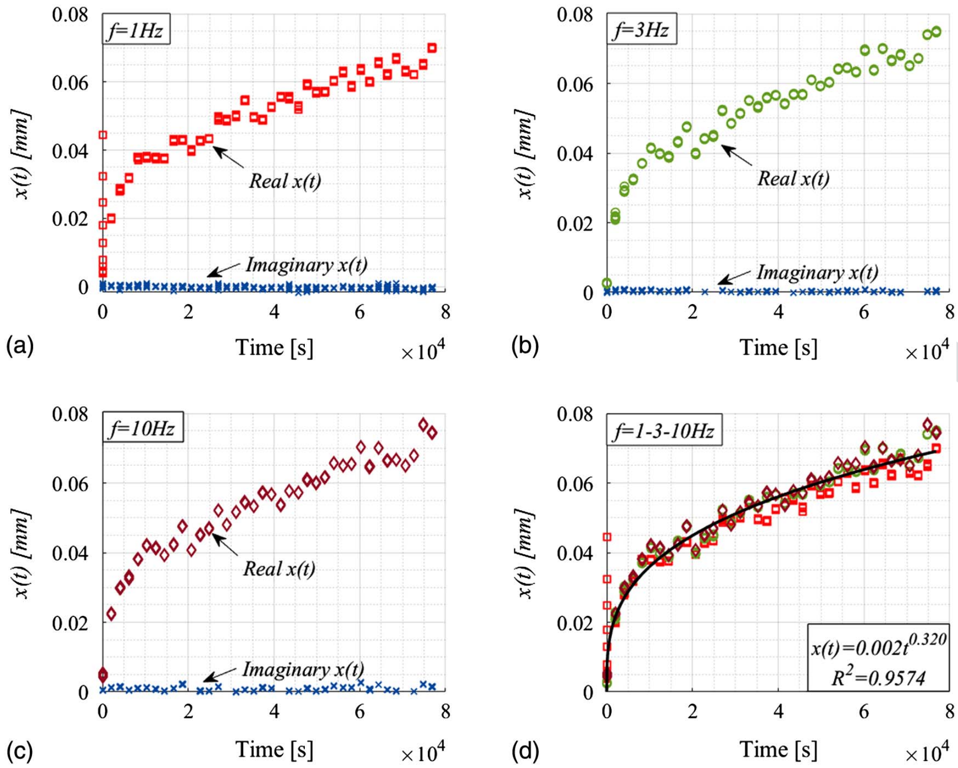

Fig. 11. (a) Evolution of the thickness $x(t)$ of the equivalent full-blend layer, showing the real part and the imaginary part as a function of time at 1 Hz; (b) evolution of the thickness $x(t)$ of the equivalent full-blend layer, showing the real part and the imaginary part as a function of time at 3 Hz; (c) evolution of the thickness $x(t)$ of the equivalent full-blend layer, showing the real part and the imaginary part as a function of time at 10 Hz; and (d) exponential regression estimated considering the data for 1, 3, and 10 Hz.

Summary and Conclusions

In this study, the diffusion phenomenon between different bitumens was characterized experimentally using a particular test protocol on single- and double-layer DSR samples and modeled using a three-layer model. The significance of this approach is the simulation of the diffusion phenomenon using only mechanical parameters, such as complex shear modulus and phase angle in the linear viscoelastic domain. The time-dependent thickness of an equivalent intermediate layer carried by diffusion was estimated and considered to be a complete homogeneous mixture of the two bitumens in equal proportions. This thickness can be considered to be the depth of the diffusion phenomenon in time. The main findings drawn from the study are the following:

- The validity of the test was proved by experimental results: single-layer and double-layer test results were compared, and there were no significant statistical differences between the two sample typologies.
- According to this model, the evaluation of the intermediate layer thickness can be considered correct, due to the frequency independence.
- This study gives an indication of the blending of two bitumens. The proposed simulation estimated the long-term behavior, through extrapolation of the model. This finding could suggest that different bitumens can interact in asphalt mixtures containing RAP. The bitumen potentially could change the rheological characteristics of the mixtures in the long term.

The results are promising for the development of a more-refined mechanical model. An extension of the experimental campaign is planned to study the effects of lower and higher temperatures and different test durations on the rheological properties of the materials within the LVE domain.

Data Availability Statement

All data, models, and code generated or used during the study appear in the published article. Some or all data, models, or code that support the findings of this study are available from the corresponding author upon reasonable request.

Acknowledgments

We thank Paolini Massimo from Valli Zabban Spa for support and the supply of the bitumens.

References

Baaj, H., M. Ech, N. Tapsoba, C. Sauzeat, and H. Di Benedetto. 2013. "Thermomechanical characterisation of asphalt mixtures modified with high contents of asphalt shingle modifier (ASM) and reclaimed asphalt pavement (RAP)." *Mater. Struct.* 46: 1747–1763. https://doi.org/10.1617/s11527-013-0015-7.

Bokstein, B. S., M. I. Mendelev, and D. J. Srolovitz. 2005. *Thermodynamics and kinetics in Material Science: A short course*. Oxford, UK: Oxford University Press.

Bonaquist, R. 2007. "Can I Run More RAP?" *HMAT: Hot Mix Asphalt Technol.* 12 (5).

Bressi, S., A. Carter, N. Bueche, and A.-G. Dumont. 2016. "Impact of different ageing levels on binder rheology." *Int. J. Pavement Eng.* 17 (5): 403–413. https://doi.org/10.1080/10298436.2014.993197.

Bressi, S., M. C. Cavalli, M. N. Partl, G. Tebaldi, A. G. Dumont, and L. D. Poulikakos. 2015a. "Particle clustering phenomena in hot asphalt mixtures with high content of reclaimed asphalt pavements." *Constr. Build. Mater.* 100 (Dec): 207–217. https://doi.org/10.1016/j.conbuildmat.2015.09.052.

Bressi, S., A. Dumont, A. Carter, and N. Bueche. 2015b. “A multiple regression model for developing a RAP binder blending chart for stiffness prediction.” In *Bituminous Mixtures and Pavements VI*, edited by A. Nikolaides, 775–783. CRC Press.

CEN (European Committee for Standardization). 2015a. *Bitumen and bituminous binders. Determination of needle penetration*. EN 1426:2015. Brussels, Belgium: CEN.

CEN (European Committee for Standardization). 2015b. *Bitumen and bituminous binders. Determination of softening point. Ring and ball method*. EN 1427:2015. Brussels, Belgium: CEN.

CEN (European Committee for Standardization). 2015c. *Bitumen and bituminous binders—Determination of the resistance to hardening under influence of heat and air—Part 1: RTFOT method*. EN 12607-1:2015. Brussels, Belgium: CEN.

CEN (European Committee for Standardization). 2018. *Bitumen and bituminous binders—Determination of dynamic viscosity of bitumen and bituminous binders by the cone and plate method*. EN 13702-1:2018. Brussels, Belgium: CEN.

Cong, P., H. Hao, Y. Zhang, W. Luo, and D. Yao. 2016. “Investigation of diffusion of rejuvenator in aged asphalt.” *Int. J. Pavement Res. Technol.* 9 (4): 280–288. https://doi.org/10.1016/j.ijprt.2016.08.001.

Ding, Y., B. Huang, X. Shu, Y. Zhang, and M. E. Woods. 2016. “Use of molecular dynamics to investigate diffusion between virgin and aged asphalt binders.” *Fuel* 174 (Jun): 267–273. https://doi.org/10.1016/j.fuel.2016.02.022.

Guo, M., Y. Tan, L. Wang, and Y. Hou. 2017. “Diffusion of asphaltene, resin, aromatic and saturate components of asphalt on mineral aggregates surface: Molecular dynamics simulation.” Supplement, *Road Mater. Pavement Des.* 18 (S3): 149–158. https://doi.org/10.1080/14680629.2017.1329870.

Jiménez del Barco Carrión, A. J. D., D. Lo Presti, and G. D. Airey. 2015. “Binder design of high RAP content hot and warm asphalt mixture wearing courses.” Supplement, *Road Mater. Pavement Des.* 16 (S1): 460–474. https://doi.org/10.1080/14680629.2015.1029707.

Kandhal, P. S. 1997. “Recycling of asphalt pavements—An overview.” *J. Assoc. Asphalt Paving Technol.* 66.

Karlsson, R., U. Isacsson, and J. Ekblad. 2007. “Rheological characterisation of bitumen diffusion.” *J. Mater. Sci.* 42 (1): 101–108. https://doi.org/10.1007/s10853-006-1047-y.

Kaseer, F., E. Arámbula-Mercado, L. Garcia Cucalon, and A. Epps Martin. 2020. “Performance of asphalt mixtures with high recycled materials content and recycling agents.” *Int. J. Pavement Eng.* 21 (7): 863–877. https://doi.org/10.1080/10298436.2018.1511990.

Kriz, P., D. L. Grant, B. A. Veloza, M. J. Gale, A. G. Blahey, J. H. Brownie, R. D. Shirts, and S. Maccarrone. 2014. “Blending and diffusion of reclaimed asphalt pavement and virgin asphalt binders.” Supplement, *Road Mater. Pavement Des.* 15 (S1): 78–112. https://doi.org/10.1080/14680629.2014.927411.

Lo Presti, D., A. Jiménez del Barco Carrión, G. Airey, and E. Hajj. 2016. “Towards 100% recycling of reclaimed asphalt in road surface courses: Binder design methodology and case studies.” *J. Cleaner Prod.* 131 (Sep): 43–51. https://doi.org/10.1016/j.jclepro.2016.05.093.

Mangiafico, S., H. Di Benedetto, C. Sauzéat, F. Olard, S. Pouget, and L. Planque. 2013. “Influence of reclaimed asphalt pavement content on complex modulus of asphalt binder blends and corresponding mixes: Experimental results and modelling.” Supplement, *Road Mater. Pavement Des.* 14 (S1): 132–148. https://doi.org/10.1080/14680629.2013.774751.

Mangiafico, S., C. Sauzéat, and H. Di Benedetto. 2019. “Comparison of different blending combinations of virgin and RAP-extracted binder: Rheological simulations and statistical analysis.” *Constr. Build. Mater.* 197 (Feb): 454–463. https://doi.org/10.1016/j.conbuildmat.2018.11.217.

Nahar, S. N., M. Mohajeri, A. J. M. Schmets, A. Scarpas, M. F. C. van de Ven, and G. Schitter. 2013. “First observation of blending-zone morphology at interface of reclaimed asphalt binder and virgin bitumen.” *Transp. Res. Rec.* 2370 (1): 1–9. https://doi.org/10.3141/2370-01.

Navaro, J., D. Bruneau, I. Drouadaine, J. Colin, A. Dony, and J. Cournet. 2012. “Observation and evaluation of the degree of blending of reclaimed asphalt concretes using microscopy image analysis.” *Constr. Build. Mater.* 37 (Dec): 135–143. https://doi.org/10.1016/j.conbuildmat.2012.07.048.

Rad, F. Y., N. R. Sefidmazgi, and H. Bahia. 2014. “Application of diffusion mechanism: Degree of blending between fresh and recycled asphalt pavement binder in dynamic shear rheometer.” *Transp. Res. Rec.* 2444 (1): 71–77. https://doi.org/10.3141/2444-08.

Shirodkar, P., Y. Mehta, A. Nolan, K. Sonpal, A. Norton, C. Tomlinson, E. Dubois, P. Sullivan, and R. Sauber. 2011. “A study to determine the degree of partial blending of reclaimed asphalt pavement (RAP) binder for high RAP hot mix asphalt.” *Constr. Build. Mater.* 25 (1): 150–155. https://doi.org/10.1016/j.conbuildmat.2010.06.045.

Wu, J., Q. Liu, S. Yang, M. Oeser, and C. Ago. 2021. “Study of migration and diffusion during the mixing process of asphalt mixtures with RAP.” *Road Mater. Pavement Des.* 22 (7): 1578–1593. https://doi.org/10.1080/14680629.2019.1710237.

Queries

1. Please provide the ASCE Membership Grades for the authors who are members.
2. Please define the acronym (LTDS).
3. Please provide author titles (e.g., Professor, Director) for 2nd affiliation of author "Stefano Noto" in affiliation footnotes.
4. Please check the hierarchy of section heading levels.
5. ASCE Open Access: Authors may choose to publish their papers through ASCE Open Access, making the paper freely available to all readers via the ASCE Library website. ASCE Open Access papers will be published under the Creative Commons-Attribution Only (CC-BY) License. The fee for this service is USD 2,000 and must be paid prior to publication. If you indicate Yes, you will receive a follow-up message with payment instructions. If you indicate No, your paper will be published in the typical subscribed-access section of the Journal. After a journal article is published, its copyright status cannot change until two years have passed. For further information, please see https://ascelibrary.org/page/openaccessoptionsandrights.
6. Please clarify whether the reference citation "Bressi et al 2015a" or "Bressi et al 2015b" throughout the article.
7. "considered as homogeneous full-blend bitumen and the degree of partial blending" is unclear. Please rewrite.
8. Please provide the manufacturer name and location (city, U.S. state or city, province, country) for product "Anton-Paar".
9. Please provide the manufacturer name and location for products "Peltier plate and Peltier hood".
10. ASCE style for math is to set all mathematical variables in italic font. Please check all math variables throughout the paper, both in equations and throughout the text, to ensure that all conform to ASCE style.
11. Please check all figures, figure citations, and figure captions to ensure they match and are in the correct order.
12. ASCE style prohibits the use of a single subsection per level. Therefore the subheading "Single-Layer versus Double-Layer Tests" was deleted.
13. "experimental results by calculations" is unclear. Please rewrite.
14. Please provide issue number for Baaj et al. (2013).
15. This query was generated by an automatic reference checking system. This reference Bonaquist (2007) could not be located in the databases used by the system. While the reference may be correct, we ask that you check it so we can provide as many links to the referenced articles as possible.
16. Please provide page range for Bonaquist (2007).
17. This reference Bressi et al. (2015a) is not mentioned anywhere in the text. ASCE style requires that entries in the References list must be cited at least once within the paper. Please indicate a place in the text, tables, or figures where we may insert a citation or indicate if the entry should be deleted from the References list.
18. Please provide publisher location for Bressi et al. (2015b).
19. This reference Bressi et al. (2015b) is not mentioned anywhere in the text. ASCE style requires that entries in the References list must be cited at least once within the paper. Please indicate a place in the text, tables, or figures where we may insert a citation or indicate if the entry should be deleted from the References list.
20. Please provide volume, issue number and page range for Kandhal (1997).
21. This query was generated by an automatic reference checking system. This reference Kandhal (1997) could not be located in the databases used by the system. While the reference may be correct, we ask that you check it so we can provide as many links to the referenced articles as possible.